ARMA 10-237

Deviation from Linear Elastic Fracture in Near-Surface Hydraulic Fracturing Experiments with Rock

Makhnenko, R.Y.
University of Minnesota, Minneapolis, MN, USA
Bunger, A.P.
CSIRO Earth Science and Resource Engineering, Clayton, Victoria, Australia
Detournay, E.
University of Minnesota, Minneapolis, MN, USA

This paper was prepared for presentation at the 44th US Rock Mechanics Symposium and 5th U.S.-Canada Rock Mechanics Symposium, held in Salt Lake City, UT June 27–30, 2010.

ABSTRACT. This paper presents the results of near-surface hydraulic fracturing experiments in a medium-grained gabbro that make use of different specimen sizes in order to observe the influence of rock heterogeneity and/or non-LEFM behavior on fracture propagation. A comparison of the results with laboratory experiments in brittle elastic materials shows that fracture paths in rock usually do not monotonically approach the free surface. Moreover, they exhibit a high degree of non-symmetry, in contrast to experiments in glass or PMMA. An attempt to correlate crack path variation among different sized specimens to a size dependent fracture toughness has been initially inconclusive due to the noise caused by these crack path complexities. Nonetheless, these results provide an initial demonstration of non-LEFM behavior in hydraulic fracturing with implications for ongoing experiments aimed at quantifying the size effect on rock fracture toughness.

1. INTRODUCTION

Laboratory tests indicate dependence of rock strength on specimen size. In particular, the nominal tensile stress associated with specimen failure decreases in an empirical power-law relationship to specimen size (e.g. [1]). This is usually explained by reasoning that tensile strength is not a true material property but depends on the specimen geometry and probable maximum flaw size that is subjected to tensile loading. Another manifestation of the size effect is expressed in the critical energy release rate associated with fracture extension — fracture energy, for short, which relates to the square of the fracture toughness — increasing usually in an empirical power-law relationship to specimen/notch/intact ligament/crack size (e.g. [2,3]). Although previous experimental works have indicated in most cases a power-law relationship at the laboratory scale (<1 m), and have led to a number of theoretical recommendations regarding the treatment of fracture in heterogeneous materials (e.g. [4,5,6,2]), how these results and theories can be appropriately extended to larger scales remains fundamentally unclear.

The overarching objective of this work is to develop a new method for estimating how the fracture toughness depends on the size of the fracture that is practically applicable at scales far exceeding laboratory limitations. It is based on hydraulically fracturing rocks at a shallow depth, that is, so that the radius of an initially horizontal, circular fracture attains a value that is several times greater than its initial depth. As these shallow hydraulic fractures grow, the asymmetry of the fracture opening induces curving of the fracture towards the surface so that the geometry resembles a concave-upward saucer. Previous research has shown that the saucer-shapes are, for homogeneous brittle materials such as glass and polymethyl methacrylate (PMMA), determined to leading order by a parameter that compares the in-situ compressive stress acting parallel to the free surface with a fracture toughness dependent estimate of the magnitude of the fracture-induced stress field [7,8,9]. Hence, these prior works show that the final saucer-shape relates directly to the fracture toughness of the material. Therefore, with knowledge of the in-situ stress field, one may in principle estimate the fracture toughness based on *a posteriori* measurements of the fracture shape and without requiring typically unreliable

measurement or analysis of the internal loading. Furthermore, this method may be applied at virtually any scale, provided one can measure the final fracture surface.

If the experiments in homogeneous brittle materials, referenced above, comprise a first step in development of this method, this paper comprises a second step. This step is to perform laboratory scale experiments in differently sized rock specimens to determine if there is evidence that the fracture toughness is a function of the specimen size at the laboratory scale, and more broadly, to determine the extent to which growth of small scale hydraulic fractures in rocks compares with homogeneous brittle elastic experiments.

2. THEORETICAL BACKGROUND

When hydraulic fractures grow near a free surface of a half-space that is not subjected to far field (or in the laboratory, applied) stresses, the fracture curves toward the surface to form a concave upward saucer wherein the radial distance from the injection point to the point at which the crack intersects the free surface, the "daylight radius" R_D, is between 3 and 4 times the initial depth H (e.g. [7,8,9,10]). It is the asymmetry in compliance between the two sides of the fracture that ultimately causes the crack path to curve towards the surface.

Existence of far field stress σ_h acting parallel to the initial plane of fracture growth reduces the fracture curving towards the free surface. In fact if σ_h is much larger than any other stress relevant to the crack growth, the optimum crack path will be horizontal in order to maintain the crack opening in the direction of the least compressive stress.

The crack path, and therefore the final shape of the saucer, is thus the result of an interaction between the crack's desire to curve, due to its asymmetry, and to remain parallel to the free surface in order to remain "properly" oriented relative to the far-field stress.

As originally suggested by Zhang et al. [11], this competition can be quantified via a dimensionless parameter that compares σ_h with the magnitude of the crack-induced, asymmetric stress field. In the context of Linear Elastic Fracture Mechanics (LEFM), the latter stress is classically estimated as $K_{Ic}/\sqrt{R}$, where K_{Ic} is the opening mode fracture toughness and R is the crack length or radius. For a shallow hydraulic fracture, $R \approx H$, where H is the initial depth. Hence, the so-called "curving parameter" χ is given by

$$\chi = \frac{\sigma_h \sqrt{H}}{K_{Ic}} \qquad (1)$$

where $\chi \to \infty$ corresponds to the case where the crack grows parallel to the surface.

The validity of χ as the parameter controlling the saucer shape has been demonstrated experimentally for homogeneous, brittle elastic materials (crack paths for different values of χ are shown in Figure 1) [7,8,9]. That is, for experiments in different materials and using differently-sized specimens, the saucer shape was found to be the same, up to a rescaling of the radial and depth coordinates by the initial depth H, provided that χ was the same from one experiment to the next.

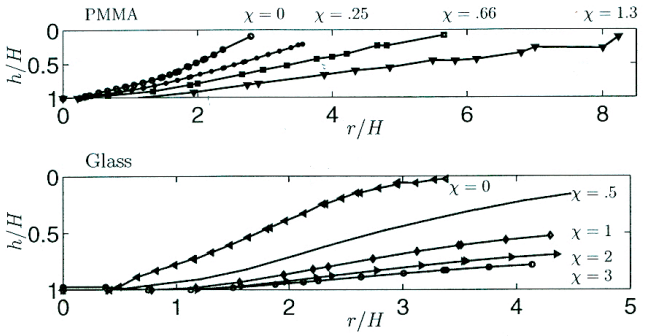

Fig. 1. Crack paths for experiments performed in PMMA and glass [8].

Hence, χ is a similarity parameter [12] governing saucer-shaped hydraulic fracture growth. However, χ is only a similarity parameter if K_{Ic} is a true material parameter, not varying with the size of the experiment or, for that matter, the stress state. But it is well known that for rocks K_{Ic} is indeed a function of the crack length. We arrive, then, to the working hypothesis underlying these experiments: For the same rock and the same nominal value of χ based on a single measured K_{Ic}, the saucer-shape resulting from shallow hydraulic fracture growth is expected to be flatter the smaller the experimental scale (i.e. for smaller H). This dependence of the saucer shape on the size would reflect the fact that the effective K_{Ic} is expected to be smaller in the smaller experiments, hence χ would be larger and the saucer shape flatter. The experiments described below are designed as an initial, laboratory-scale test of this hypothesis.

3. EXPERIMENTAL OVERVIEW

Saucer-shaped hydraulic fractures were created in block-shaped specimens of a medium-grained (~2 mm grain size) gabbro, commercially known as Adelaide Black Granite, by injecting glycerin solutions at a constant rate using a positive displacement stepping motor pump, as shown in Figure 2. The fractures were initiated from a

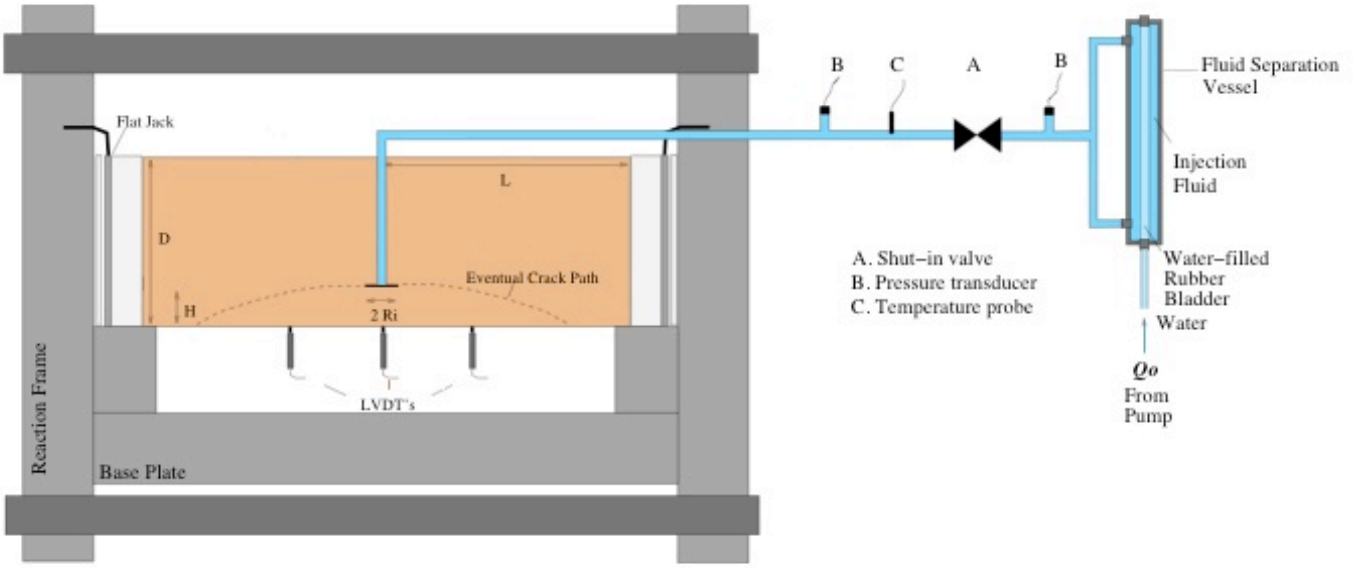

Fig 2. Cross-section of the setup for the laboratory experiments.

0.5-2 mm deep circumferential notch at the base of a hole that terminated a prescribed distance from the blocks' surface. In each case, a stainless steel tube was epoxy cemented into the hole, connected to the pump, and thus used to deliver the fluid to the notch. Upon commencing pumping, the pressure would increase to breakdown, after which the hydraulic fracture would grow from the notch while the injection pressure decreased. Finally, the fracture reached either the bottom surface or one of the sides of the block, at which point the pumping ceased and the test was completed..

Three main design criteria were used. Firstly, the experiments were designed so that the average or maximum hydraulic fracture radius attained in a test, which is a function of the initial depth H (Figure 2), would vary relative to the grain size in the rock. For example, Mulmule and Dempsey [13] observed a size effect on K_{Ic} in sea ice when the crack size was less than about 200 times the largest grain size. In our case, investigation of the effect of varying of the crack size relative to the grain size makes use of two block sizes: small (200×200×120 mm, $H = 22$ mm, hole diameter 8.6 mm) and medium (400×400×235 mm, $H = 45$ mm, hole diameter 18.3 mm). Hence the maximum crack radius is circa 50 times the grain size for the small blocks and 100 times the grain size in the large blocks.

The second experimental design criterion is to ensure so-called physical similarity [12], by keeping the parameter χ from equation (1) the same between comparable tests in the small and medium blocks. Here σ_h is the horizontal stress applied using water-filled stainless steel flat jacks and K_{Ic} is the fracture toughness. Note that the nominal value for K_{Ic} was found using semi-circular beam tests [14] to be in the range of $1.27 - 2.98$ MPa$\sqrt{\text{m}}$, increasing with specimen size, with the notch length ranging from 1.5-14 mm.

Finally, we wanted to ensure that the influence of viscous flow can be neglected, such that all the experiments were run in a so-called toughness-dominated regime, which requires the experimental duration to far exceed a characteristic time associated with the fracture's transition from the viscosity to toughness dominated regime, given by [15]

$$t_{mk} \simeq 0.0145 \left(\frac{\mu^5 Q_0^3 E'^{13}}{K_{Ic}^{18}} \right)^{1/2} \qquad (2)$$

For these experiments, $0.79 \le Q_0 \le 3.0$ mm^3/sec is the constant injection rate, $E' = E/(1-\nu^2)$ for Young's modulus $E = 91$GPa and Poisson's ratio $\nu = 0.30$, and $\mu = 0.83$Pa$\cdot$sec is the dynamic viscosity of the glycerin solution at the usual experimental temperature of 19^0C. Hence, we obtain $t_{mk} < 0.05$ sec for these experiments that always lasted more than 5 seconds, which ensures that they are conducted in the toughness-dominated regime.

In addition to monitoring the injection pressure and pumping rate, the surface displacement associated with hydraulic fracture growth was measured using an array of linear variable differential transformers (LVDTs): one central and four peripheral, which are sketched in Figure 2.

4. EXPERIMENTAL RESULTS

4.1. Pressure and displacement response

When injection commenced, the pressure increases prior to the beginning of fracture growth. Once the injection pressure reaches about 4 MPa, the pressure increases approximately linearly with time, with the slope proportional to the injection rate and inversely proportional to the compliance of the injection system. Eventually crack growth begins, where the pressure required is a function of the strength of the rock, the applied stresses, the size and sharpness of the initial notch, the injection rate, and the viscosity of the fluid.

The first graph in Figure 3 shows the injection pressure versus time along with the LVDT-measured displacement on the surface at the nominal fracture center, that is, directly opposed to the injection tube location. For this example, at 1600 seconds the injection rate was decreased, accounting for the change in slope at this time. The second graph in Figure 3 shows the surface displacement rate as a function of time. The point where the injection was stopped (3058 sec) is clearly visible in this graph. Throughout the initial pressurization the surface displacement increases slowly and nearly linearly. The surface displacement has an upward inflection, which is interpreted as the beginning of crack growth, at about 2890 sec (the vertical black line in Figure 3), while the pressure increases to finally reach a maximum at about 2960 sec. During this time we infer that the fracture is indeed growing but with the injection pressure increasing. In previous research, the peak pressure exceeding the crack initiation pressure is a phenomenon that has been associated through modeling and theoretical considerations with growth of the hydraulic fracture through the varying near-wellbore stress field [16], the compressibility of the injection system [17], and both of these mechanisms combined with viscous fluid flow [18]. It was previously observed in hydraulic fracturing experiments in rocks by Zhao et al. [19], who also observe an increase of the breakdown pressure with pressurization rate, and with decreasing the borehole radius [20].

While it can be inferred that crack initiation significantly precedes the system reaching the peak pressure for the example of test 15M, and indeed, for all tests in medium sized blocks, this behavior is apparently not present in the smaller blocks. Figure 4 shows the injection pressure, surface displacement at the crack center and the displacement rate for the small block, test 10S. The time of the first upward inflection in the surface displacement curve is indistinguishable from the time of the peak pressure.

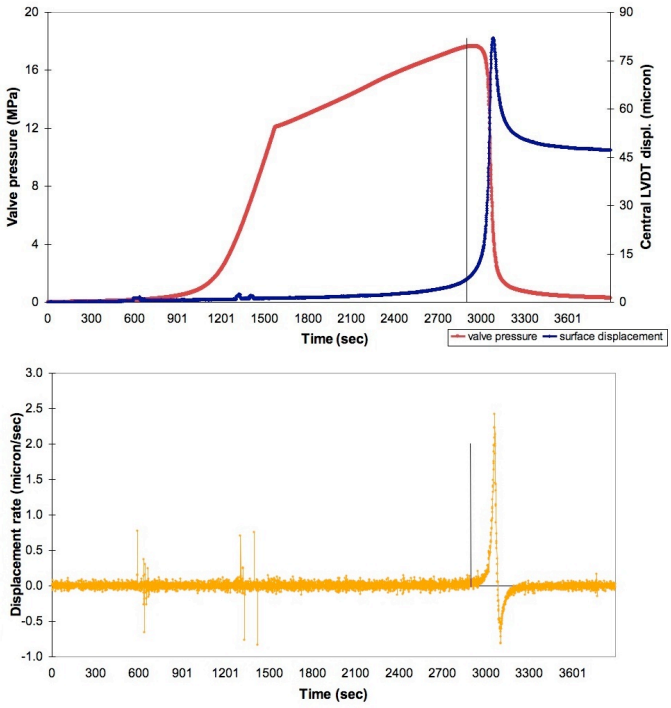

Fig. 3. Valve pressure, central LVDT displacement and displacement rate vs experimental time for Test 15M.

To explain this difference between the medium and small blocks, we turn to numerical modelling for a plane strain hydraulic fracture. Reference [18] has shown that, among other factors, the difference between the crack initiation and peak pressure increases when the initial notch depth increases relative to a certain length scale that is smaller when the injection system compressibility is smaller. In these experiments, the notches were typically able to be made deeper for the medium blocks (3-5 mm deep) than for the small blocks (1-1.5 mm deep). Also, examination of the linear portion of the pressure versus time plots indicates that the injection system was less compressible in the case of the medium blocks. Hence, it is consistent with previous numerical predictions [16,18] that the medium size blocks would exhibit crack initiation that clearly precedes the peak pressure while the small blocks do not.

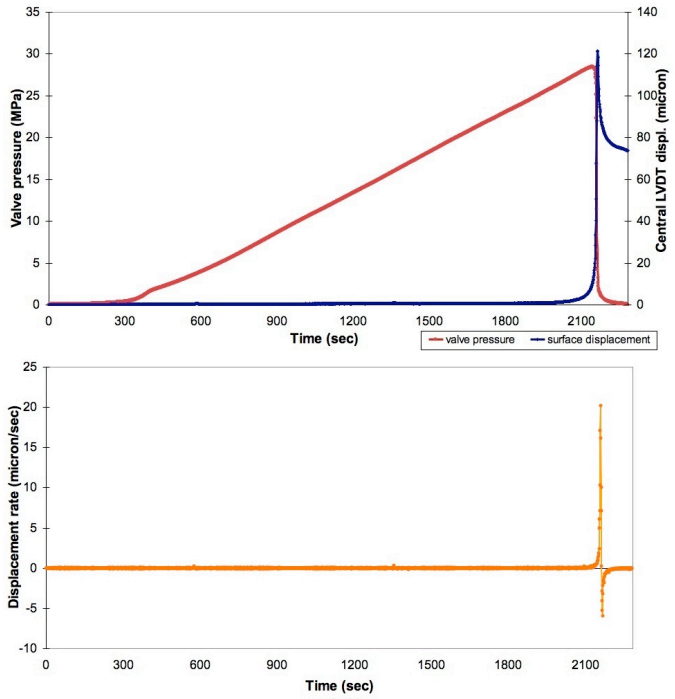

Fig. 4. Valve pressure, central LVDT displacement and displacement rate vs experimental time for Test 10S.

4.2. Crack paths analysis

The objective of these experiments is to compare the crack paths in rock specimens with those from homogeneous linear elastic specimens with the same value of the parameter χ. To this end, the value of the fracture toughness ($K_{Ic} = 2.84\,\mathrm{MPa}\sqrt{\mathrm{m}}$) for the largest size semi-circular beam tests (with diameters equal to 90mm and 30mm thick) was taken to calculate the nominal values of χ (χ_{nom}) from Eq. (1). These values together with the values of applied confined stress (σ_r), distance from the initial notch to the specimen surface (H), and injection rates (Q_0) are presented in Table 1.

Table 1. Values of σ_r, H, Q_0 and χ_{nom} for conducted experiments.

Exp. ID	σ_r [MPa]	H [mm]	Q_0 [mm^3 / sec]	χ_{nom}
5S	5.04	23	3.00	0.27
7S	15.18	21.8	2.37	0.79
8S	8.96	22.3	2.37	0.47
9S	4.56	23.2	2.37	0.25
10S	5.65	23.7	2.37	0.31
11S	7.79	21.2	2.37	0.40
12M	5.22	43.6	2.37	0.38
13M	10.10	46.2	1.58	0.76
14M	6.13	47.4	0.79	0.47
15M	3.35	43.2	0.79	0.25

Note that characters "S" and "M" are related to the tests with small size and medium size blocks respectively. Experiments 12M, 13M, 14M, and 15M have approximately the same values of χ_{nom} as experiments 11S, 7S, 8S, and 9S respectively.

The shape of the crack surface was determined by direct measurements - each block was cut through the borehole in four directions: East, North, West, and South relative to the blocks orientation as it was placed in the polyaxial compression frame (half of the block 12M with saw cut in North direction is shown in Figure 5). Then, these paths were plotted in dimensionless radius (R/H) and dimensionless fracture depth (h/H) coordinates and were contrasted with the LEFM experimental crack paths with the same value of χ_{nom}. Data from glass and PMMA (considered as linearly elastic materials) near surface hydraulic fracturing tests described in [8] was taken for this comparison.

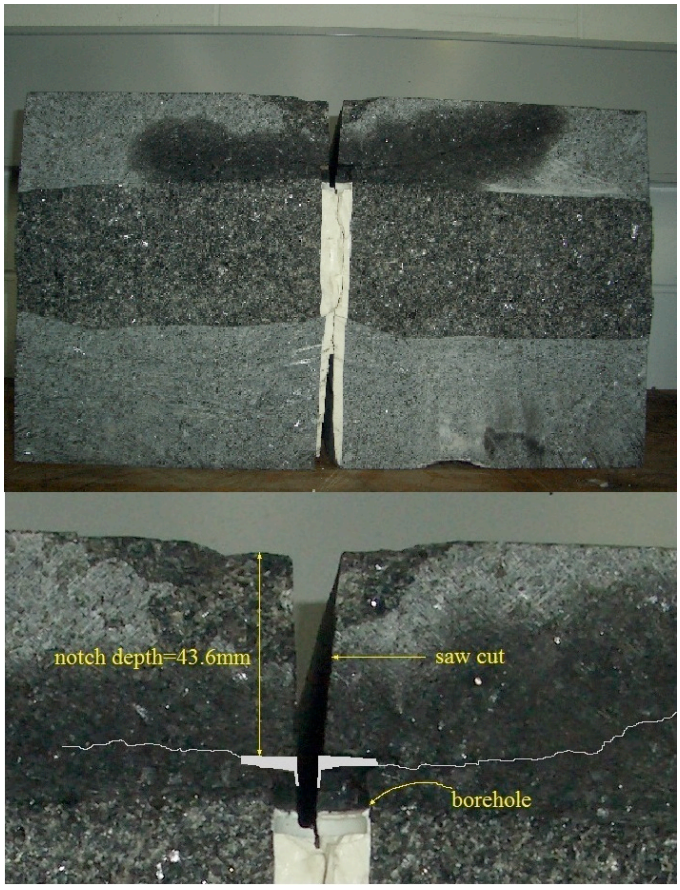

Fig. 5. Block 12M cut in half (top) and a close-up of the central part (bottom) with the highlighted notch and fracture paths.

In the LEFM cases, the crack paths measured in different directions were observed to be highly consistent with one another. The only appreciable asymmetry in the LEFM experiments came in the form of the initially circular hydraulic fracture eventually favoring propagation in one direction to the detriment of the others so that the final plan-view shape of the fracture

was egg-shaped rather than circular. Additionally, in the LEFM cases, the fracture reaches the surface ("daylighted") over only a small portion of its leading edge due to this late-stage asymmetry [8,9].

Test 8S closely mimicked this LEFM behavior. Figure 6 depicts the path measured in four radial directions as well as the curve for the average crack path for one of the Glass tests from [8], with the nominal value of χ ($\chi = 0.50$). One can see that for Test 8S all four measured crack paths are almost the same in terms of their shape and length; the only significant difference is that the fracture daylighted in the West direction and, correspondingly, propagated longer in this direction. Reasonable consistency among the fracture paths in different directions was also observed for test 5S (Figure 7), although to a lesser degree than Test 8S.

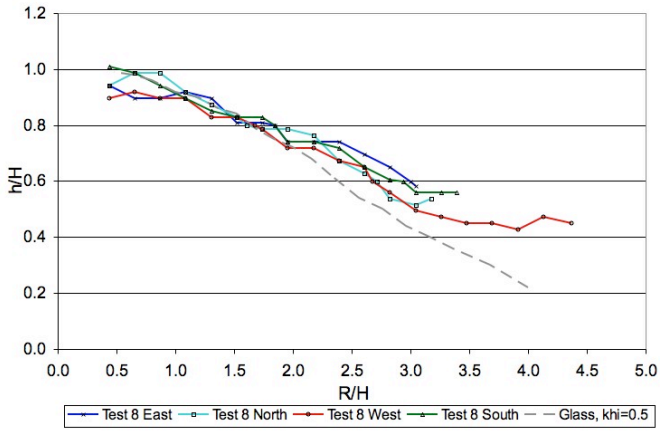

Figure 6. Fracture paths in four directions for test 8S.

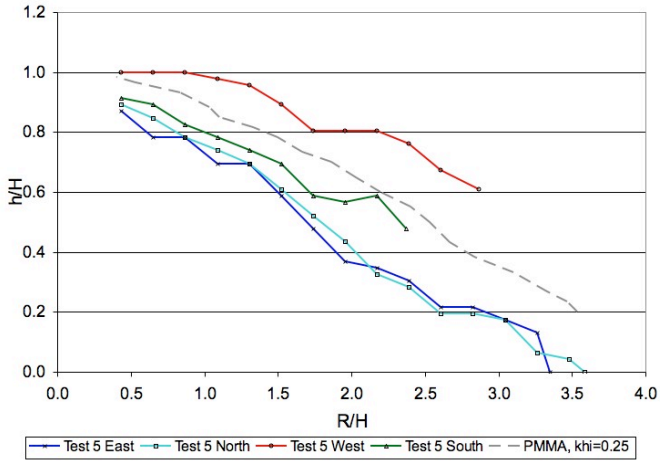

Figure 7. Fracture paths in four directions for test 5S.

For the other tests, some notable differences between fracture paths shapes and lengths in different directions were observed. Figures 8-10 demonstrate these observations for tests 12M, 14M, and 10S. Typically the corresponding crack path for the same value of χ from the LEFM experiment for each test was situated between the paths in four directions, even if the deviation of the crack paths from the LEFM experimental crack path varied significantly.

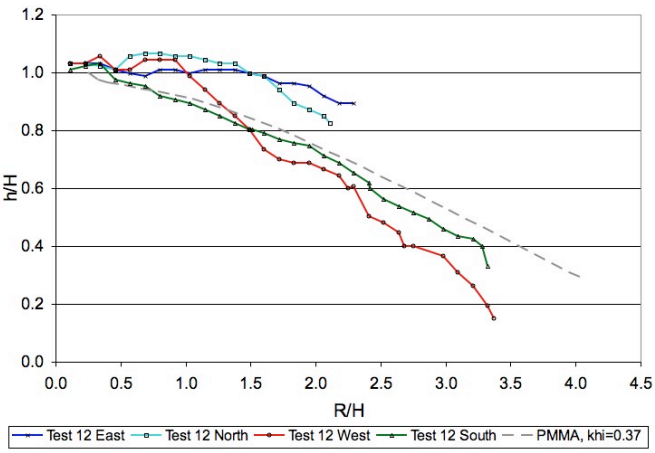

Figure 8. Fracture paths in four directions for test 12M.

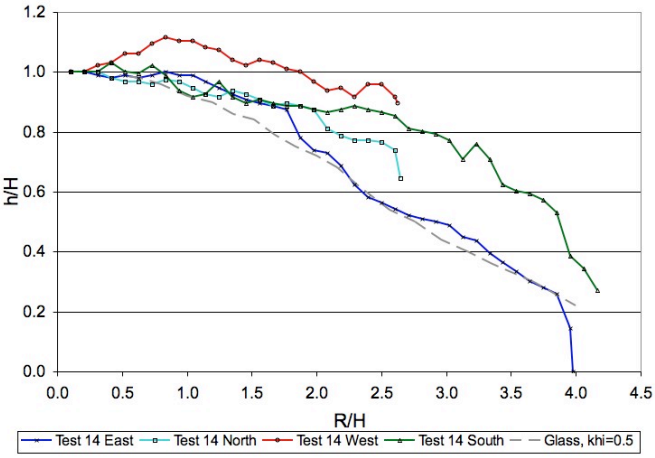

Figure 9. Fracture paths in four directions for test 14M.

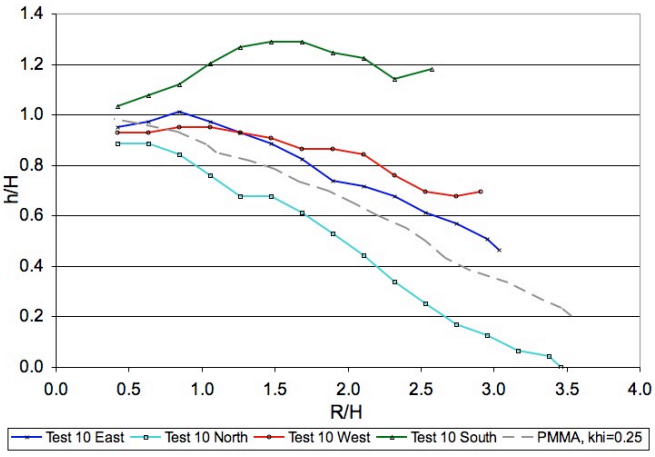

Figure 10. Fracture paths in four directions for test 10S.

The following procedure was implemented to calculate the experimental values of K_{Ic} for each test. Figure 11 shows the relation between χ and the radius to depth ratio, R/H, corresponding to different values of h/H, where h is the depth of the fracture surface and H is the initial depth. Hence, the curve $h/H = 0$

corresponds to R/H when the fracture intersects the surface, or daylights; the curve $h/H = 0.2$ corresponds to R/H when the fracture surface is 20 percent of the initial depth away from the free surface, and so forth. So, the goal of the proposed method is to use curves from Figure 11 to obtain the average value of χ given R/H at various values of h/H (0.8, 0.6, 0.4, 0.2, and 0). As χ satisfies Eq. (1), given the initial depth and the in-situ stress, one may estimate K_{Ic} directly.

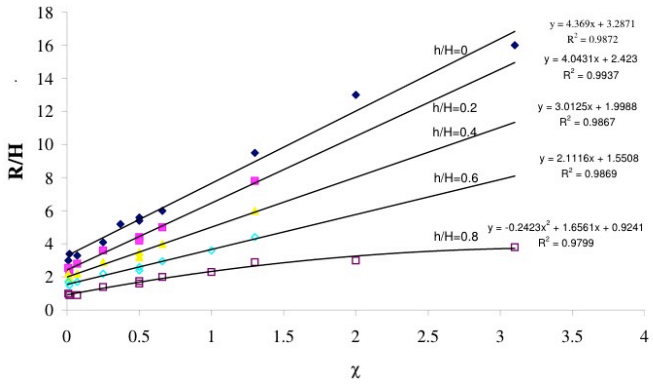

Figure 11. Relation between normalized radius and χ at various normalized depths determined by analysis of curving crack surfaces for glass and PMMA.

Calculated values of χ in four directions (East, North, West, and South), which are the arithmetic means of the fitted χ at five h/H values listed above, are shown in Table 2; the gaps for some tests represent the directions in which fractures did not propagate far enough to allow us to estimate the related χ values. Values of the stress intensity factor K_{Ic} were calculated using the average (or "best fit") value of χ (χ_{av}) for each test.

Table 2. Values of χ at four different directions for experiments 5S,7S-11S,12M-15M.

Exp. ID	East	North	West	South	χ_{av}	K_{Ic} [MPa$\sqrt{\text{m}}$]
5S	0.03	0.02	0.59	0.07	0.18	4.24
7S	0.71	0.37	1.19	-	0.76	2.95
8S	0.69	0.57	0.55	0.68	0.62	2.16
9S	0.14	-	0.45	-	0.30	2.32
10S	0.50	0.05	0.90	-	0.48	1.81
11S	0.47	0.40	0.20	0.16	0.31	3.66
12M	-	-	0.31	0.41	0.35	3.11
13M	-	-	0.42	-	0.42	5.16
14M	0.38	0.86	-	0.99	0.74	1.81
15M	0.37	-	0.51	0.06	0.31	2.25

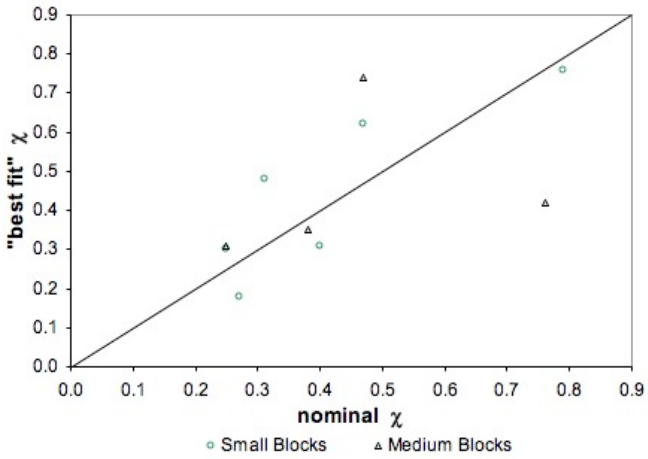

Figure 12.The "best fit" values of χ vs the nominal χ values for tests 5S,7S-11S,12M-15M.

Then, the "best fit" values of χ versus the nominal values were plotted to observe the correlation between them (Figure 12). Recall that the working hypothesis states that K_{Ic} increases with the size of the crack, that is the size of the experiment, and that this will be expressed by saucers that curve more strongly and therefore have smaller "best fit" values of χ than the nominal values. And further, this tendency is proposed to be stronger for the medium blocks than the small blocks.

In actuality, one can see that there is no clear correlation between the nominal and "best fit" χ values. Some experiments fall above $\chi_{nom} = \chi_{av}$ line, some below. And it does not depend on the size of the block: both small blocks and medium blocks tests have the "best fit" χ values below and above the line. Whatever systematic variation there is in χ due to the size effect on the fracture toughness would appear to be masked by other factors that all lead to the observed scatter of the experimental results when viewed in this way. Why are the results so scattered? A couple of suggestions can be put forward:

(i) Both the size effect on K_{Ic} that is under investigation and the crack path variation (Figures 8-10) that leads to imprecise estimation of χ have the same origin, that is, the heterogeneity of the rock. In order to perform experiments at an "interesting" range of sizes from the perspective of the size effect, they cannot be too large relative to the size of the heterogeneities. However, at this scale the small scale fluctuations in stress, pre-existing planes of weakness, and variability of material properties among the crystals also cause significant crack path variability. This issue could be a significant detriment to this approach for investigating size effect if one cannot find a suitable intermediate range of specimen sizes

where the size effect on K_{Ic} is observable but the heterogeneity scale is small enough to not strongly affect the crack paths.

(ii) The initial notch is relatively blunt - around a couple of millimeters in opening. Upon inspection we see that the fracture can grow from the top of the notch, the bottom of the notch, or in between (e.g. Figure 5 and Figure 10). This initial point of crack growth significantly influences the direction of further fracture propagation and, hence, the final value of measured χ in each direction.

It is clear, then, that if the size effect on fracture toughness is to be observed and measured using shallow saucer-shaped hydraulic fracturing experiments, some additional considerations must be accounted. A wider range of block sizes relative to the size of the heterogeneities in the rock would potentially address issue (i) by firstly giving the possibility for a wider range of variation of χ, thus increasing the strength of the hypothesized systematic response. Secondly, by examining a wider range of block sizes one may find a suitable intermediate size range that satisfies the simultaneous requirement that the size effect is observable over the range of sizes but the crack paths are not too noisy due to the influence of the heterogeneities. At least one could more definitively determine if such an ideal intermediate scale exists. Issue (ii) is, in some ways, more difficult to address as there are practical limitation on how sharp and deep one can cut a notch inside a borehole in a laboratory rock specimen. However, in addition to developing tools to make the notch as sharp as possible, increasing the specimen size so that this initial variation of initiation depth and direction is smaller relative to the overall size of the experiment would be expected to improve the experimental results.

5. CONCLUSIONS

The experimental study was conducted on near-surface hydraulic fracturing in medium-grained gabbro specimens of two different sizes. The critical pressures at which hydraulic fractures initiate and the paths of the propagated fractures were investigated. The following things were found:

- The effect of the peak pressure exceeding the crack initiation pressure was observed in the tests with medium sized blocks, but was indistinguishable for small sized blocks.
- For most of the tests, fracture paths were significantly different in four directions investigated and deviated from LEFM experimental curves.
- The absence of clear correlation between nominal values of dimensionless parameter χ, governing the fracture curvature, and its experimental "best fit" values was found, which was to the detriment of the method for investigation of the size effect on rock fracture toughness over the range of specimen sizes considered.

The experimental results presented here suggest that wider range of block sizes relative to the size of the heterogeneities in the rock has to be investigated. It should provide one with a wider range of variation of χ, making it possible to find a suitable intermediate size range that satisfies the requirement that the size effect is observable over the range of sizes but the crack paths are not too noisy due to the influence of the heterogeneities.

ACKNOWLEDGMENTS

R. Makhnenko and E. Detournay gratefully acknowledge support from the National Science Foundation under Grant No. 0600058. Any opinions, findings, and conclusions or recommendations expressed in this material are those of the authors and do not necessarily reflect the views of the National Science Foundation.

REFERENCES

1. Hobbs, D.W. 1965. An assessment of a technique for determining the tensile strength of rock. *Brit. J. Appl. Phys*. 16:259-269.
2. Carpinteri, A. 1994. Scaling laws and renormalization groups for strength and toughness of disordered materials. *Int.J. Solids Struct.* 31(3):291-302.
3. Shlyapobersky, J., Mo.A. Issa, Ma.A. Issa, MD.S. Islam, J.W. Dudley, Y. Shulkin, and A. Chudnovsky. 1998. Scale effects on fracture growth resistance in poroelastic materials. In *Proceedings of SPE Annual Technical Conference and Exhibition, New Orleans, 27-30 September 1998*, SPE 48929.
4. Borodich, F.M. 1999. Fractals and fractal scaling in fracture mechanics. *Int. J. Fracture* 95:239-259.
5. Bazant, Z.M. 1997. Scaling of quasibrittle fracture: asymptotic analysis. *Int. J. Fracture* 83:19-40.
6. Dyskin, A.V. 1997. Crack growth criteria incorporating non-singular stresses: Size effect in apparent fracture toughness. *Int. J. Fracture* 83:193-206.
7. Bunger, A.P., R.G. Jeffrey, and E. Detournay. 2008. Evolution and morphology of saucer-shaped sills in analog experiments. In *Structure and Emplacement of High-Level Magmatic Systems*, ed. K. Thompson and N. Petford, 302:107–118.
8. Bunger, A.P. 2005. *Near-Surface Hydraulic Fracture. PhD thesis*. University of Minnesota, Minneapolis, MN.

9. Bunger, A.P., R.G. Jeffrey, and E. Detournay. 2004. Toughness-dominated near-surface hydraulic fracture experiments. In *Gulf Rocks 2004 - Proceedings of the Sixth North American Rock Mechanics Symposium, Houston, 5-12 June 2004*, eds. D. Yale et. al, paper No. 468.

10. Fialko, Y. 2001. On origin of near-axis volcanism and faulting at fast spreading mid-ocean ridges. *Earth Planet Sc. Lett.* 190:31-39.

11. Zhang, X., E. Detournay, and R.G. Jeffrey. 2002. Propagation of a penny-shaped hydraulic fracture parallel to the free-surface of an elastic half-space. *Int. J. Fracture* 115:125-158.

12. Barenblatt, G.I. 1996. *Scaling, Self-Similarity, and Intermediate Asymptotics,* volume 14 of *Cambridge Texts in Applied Mathematics*. Cambridge UK: Cambridge University Press.

13. Mulmule, S.V., and J.P. Dempsey. 2000. LEFM size requirements for the fracture testing of sea ice. *Int. J. Fracture* 102:85-98.

14. Lim, I.L., I.W. Johnston and S.K. Choi. 1993. Stress intensity factors for semi-circular specimens under three-point bending. *Engng Frac. Mech.* 44(3): 363-382.

15. A. Savitski, A., and E. Detournay. 2002. Propagation of a penny-shaped fluid-driven fracture in an impermeable rock: asymptotic solutions. *Int. J. Solids Struct.* 39:6311-6337.

16. Detournay, E., and R. Carbonell. 1997. Fracture-mechanics analysis of the breakdown process in minifracture or leakoff test. *SPE Production and Facilities*, August, pp. 195-199. (SPE 28076).

17. Ito, T., A. Sato, K. Hayashi. 1997. Two methods for hydraulic fracturing stress measurements needless the ambiguous reopening pressure. *Int. J. Rock Mech. & Min. Sci.* 34:3-4, paper No. 143.

18. A. Lakirouhani, A. Bunger and E. Detournay. 2008. Modeling initiation of hydraulic fractures from a wellbore. In *Proceedings of 5th Asian Rock Mechanics Symposium*, *Tehran, Iran, 24-26 November 2008*. 1101-1108.

19. Zhao, Z., H. Kim, and B. Haimson. 1996. Hydraulic fracturing initiation in granite. In *Rock Mechanics: Tools and Techniques*, eds. Aubertin, Hassani & Mitri, 1279-1284.

20. Haimson, B. and Z.Zhao. 1991. Effect of borehole size and pressurization rate on hydraulic fracturing breakdown pressure. In *Proceedings of 32nd U.S. Symposium on Rock Mechanics, Norman OK 10-12 July 1991*. 191-199. Rotterdam: Balkema.